Non-stationary quasi-periodic pulsations in solar and stellar flares

Non-stationary quasi-periodic pulsations in solar and stellar flares

V. M. Nakariakov[1,2], D. Y. Kolotkov[1], E. G. Kupriyanova[3], T. Mehta[1], C. E. Pugh[1], D.-H. Lee[2], A.-M. Broomhall[1]

[1] Centre for Fusion, Space and Astrophysics, Physics Department, University of Warwick, Coventry CV4 7AL, United Kingdom
[2] School of Space Research, Kyung Hee University, Yongin, 446-701, Gyeonggi, Korea
[3] Central Astronomical Observatory at Pulkovo of the Russian Academy of Sciences, St. Petersburg, Russia

E-mail: V.Nakariakov@warwick.ac.uk

August 2018

Abstract. Often the enhanced electromagnetic radiation generated in solar and stellar flares shows a pronounced (quasi)-oscillatory pattern — quasi-periodic pulsations (QPP), with characteristic periods ranging from a fraction of a second to several tens of minutes. We review recent advances in the empirical study of QPP in solar and stellar flares, addressing the intrinsic non-stationarity of the signal, i.e. the variation of its amplitude, period or phase with time. This non-stationarity could form a basis for a classification of QPP, necessary for revealing specific physical mechanisms responsible for their appearance. We could identify two possible classes of QPP, decaying harmonic oscillations, and trains of symmetric triangular pulsations. Apparent similarities between QPP and irregular geomagnetic pulsations Pi offer a promising avenue for the knowledge transfer in both analytical techniques and theory. Attention is also paid to the effect of the flare trend on the detection and analysis of QPP.

PACS numbers: 52.35.Bj, 52.35.Mw, 52.35.Vd, 95.30.Qd, 96.60.qe, 97.10.Jb

1. Introduction

Solar flares are impulsive, usually lasting less than a few hours, releases of energy of the magnetic field generated in the Sun. Together with coronal mass ejections, flares are the most powerful physical processes in the solar system, which affect the whole heliosphere. From the point of view of plasma physics, the flaring sites are natural plasma laboratories for the comprehensive study of basic plasma processes, such as magnetic reconnection, acceleration of charged particles, various kinds of wave motions, interaction of electron beams with the background plasma, transport processes, shocks, and many others (see [1, 2] for comprehensive reviews of theory and observations, respectively). Apparently similar energy releases are observed on other stars, including those similar to the Sun (e.g., [3]). The strongest stellar flares are often referred to as "superflares", as they are several orders of magnitude more powerful than the strongest solar flares observed so far (e.g., [4]). The interest in stellar superflares is connected, in particular, with the question of whether the Sun is also able to produce a superflare, which could be devastating for our civilisation, and, more generally, with the extension of the range of flaring parameters. However, there is still a question of whether solar flares and stellar superflares are caused by the same physical mechanism.

A prevalent but still poorly understood feature of solar and stellar flares are quasi-periodic pulsations (QPP) of the emission. In observations of the Sun as a star, i.e. without spatial resolution, as well as intrinsically in stellar observations, QPP are seen as quasi-periodic time variations of the emission curves called lightcurves, see Fig. 1 for an example. There is no rigorous definition of a QPP, but intuitively it can be thought of as a time-varying signal with a characteristic time scale. This vague definition excludes the variability associated with coloured noise or power-law spectra, while it does include quasi-monochromatic and modulated oscillatory signals.

In the spatially-resolved observations of the Sun, it is possible to identify the location of the modulated emission source. The first detection of a QPP pattern simultaneously in the X-ray and microwave emission of a solar flare was published almost fifty years ago in [5]. QPP are detected in different phases of flares, and in all observational bands, from radio to gamma-rays. QPP are detected in the light curves associated with both thermal and non-thermal emission mechanisms. One important exception is the lack of the detection of QPP in solar flares in the white light emission, while QPP are confidently detected in this band in stellar flares. However, we should point out that solar flares are rarely detected in the white light anyway, see [6] for a recent discussion.

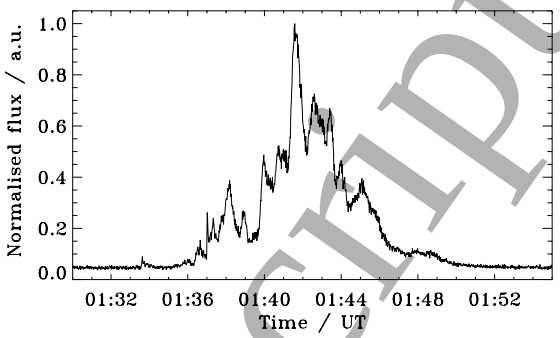

Figure 1. Example of a light curve with a pronounced QPP pattern, showing an X2.1-class solar flare SOL2013-05-15T01:45, observed with Fermi/GBM in the 50-100 keV hard X-ray waveband.

Until recently, QPP have been studied in individual flares with the use of various, often *ad hoc* techniques‡. Recent commissioning of the new generation of space-borne and ground-based instruments that provide an almost uninterrupted monitoring of the Sun, allowed for statistical studies of QPP. It was established that QPP are a statistically significant feature of solar flares in both non-thermal [7] and thermal [8, 9] emission. This conclusion excludes the possible occurrence of apparent QPP because of the red noise or the superposition of multiple unrelated flares. The estimated fraction of flares with detected QPP differs significantly in different studies, reaching 90% for major flares [9]. More conservative analytical techniques reduce this fraction to 8–30% [10, 11]. The fraction of stellar flares with confidently detected QPP is smaller, only a few percents [12], while still statistically significant. The relative rareness of the QPP detection is stellar flares could be attributed

‡ A collection of published case studies, possibly incomplete, could be found online, warwick.ac.uk/fac/sci/physics/research/cfsa/people/valery/research/qpp

to the low signal-to-noise ratio, the instrumental sensitivity and resolution, and the limitation of the analytical techniques.

The relationship of QPP parameters to properties of the host active regions has not been established. For example, the weak correlation of QPP periods with the flare amplitude and duration, found in [11], was concluded to likely be caused by an observational bias. No correlations were found with the active region area, magnetic bipole separation distance at the solar surface, or average magnetic field strength. Likewise, no dependence of the QPP period on the flare longitude or the flare class was revealed [9]. Analysis of QPP in the white light emission of stellar flares showed no correlation between the QPP period and the stellar temperatures, radii, rotation periods and surface gravity, and the flare energy [12].

The interest in QPP was reinforced by the direct detection of magnetohydrodynamic (MHD) waves and oscillations in the solar corona, with both the oscillation period and wavelength being well resolved (e.g. [13]). Indeed, the typical periods of QPP, ranging from a second to several minutes (e.g. [14]), coincides with the periods of MHD oscillations in various plasma structures of the corona. Hence, it is natural to assume that, at least in some cases, QPP are produced by the modulation of the flaring emission by MHD oscillations. The emission modulation could be produced either directly, by the variation of the macroscopic plasma parameters in the MHD wave, or indirectly, by the modulation of the reconnection rate or electron acceleration or kinematics (see, e.g., [15] for a review). However, in some cases the association of QPP with MHD oscillations is not convincing, as the detected QPP periods are significantly different from the MHD wave travel times in the host active regions. Also, the QPP modulation depth often reaches 100% of the background flare trend, while the typical relative amplitudes of coronal MHD waves are usually lower than 5–10%. Another popular interpretation of QPP is connected with self-oscillatory processes in the flaring site, which could be referred to as "magnetic dripping" e.g., repetitive magnetic reconnection. However, this interpretation has certain difficulties too, as numerical simulations show that magnetic reconnection is characterised by power-law distributions (e.g., [16, 17]), and hence does not have a characteristic time scale. Thus, the physical mechanisms for QPP are still under investigation. Evolution of our understanding of the QPP theory could be traced by the series of reviews [15, 18, 19, 14].

The mechanisms of both kinds, based on MHD oscillations and self-oscillations, are capable producing QPP with non-stationary properties. In the mechanisms based on oscillations, the oscillation amplitude and period vary because of the dissipation and variation of the parameters of the plasma and geometry of the oscillating plasma structure. For example, in the case of sausage oscillations, the period modulation could be caused by the variation of the width of the oscillating coronal loop and the steepness of its transverse profile (e.g., [20]). Likewise, the decrease in the loop length caused by flaring shrinking decreases the kink oscillation period (e.g. [21, 22]). Also, variation of the plasma temperature, for example, because of the radiative or thermal conductive cooling in the decaying phase of the flare, should increase the period of slow magnetoacoustic oscillations (e.g., [23]). In self-oscillations, e.g., the repetitive reconnection, the characteristic times could change, for example, because of the variation of the inflow rate, the anomalous resistivity connected with the local electric currents, etc. However, the intrinsic non-stationarity of QPP, predicted by the theory, has received little attention so far. In this paper we review the recent advances in the empirical study of QPP in solar and stellar flares, addressing the intrinsic non-stationarity of the signal.

2. QPP detection and analysis

2.1. Non-stationarity of QPP signals

Fig. 2 shows an example of a light curve with apparently non-stationary QPP, and the detrended QPP pattern. The effective quality factor of the QPP could be defined as the number of the oscillation cycles in the QPP pattern. Obviously, one should count only those oscillation cycles whose instantaneous amplitudes exceed some threshold value, for example, of one third of the highest amplitude in the QPP. Fig. 3 shows the statistics of this effective quality estimated for the QPP events that occurred in the same long-lived solar active region and described in [11]. In addition, the right panel of Fig. 3 shows the lack of the dependence of the number of oscillation cycles on the mean period. The typical duration of a QPP pattern is only a few oscillation cycles. Thus, a QPP is rather a wavelet or a non-stationary "oscillation burst". This intrinsic feature must be taken into account in its detection and analysis. We would like to stress that in the QPP wavelet both the amplitude and period can be heavily modulated, and thus one should not consider a QPP as a product of a harmonic function with a certain envelope function. In other words, QPP patterns are essentially non-stationary oscillations, making the results of the Fourier-based detection and analysis techniques questionable. An additional inherent complication is the inability of spectral methods to distinguish between whether the signal non-stationarity is caused by the variation of the amplitude or variation of the frequency (see, e.g.,

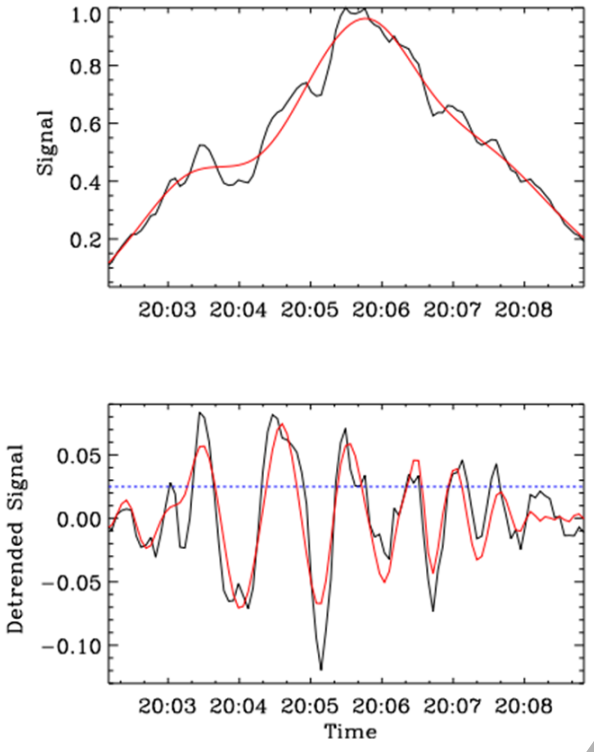

Figure 2. Top panel: Lightcurve of the solar flare SOL2014-10-27T20:03, recorded with Fermi in the 50–100 keV channel (black curve), and the trend determined by the Empirical Mode Decomposition technique. Bottom panel: Detrended signal (black) and its intrinsic mode (red). The blue dashed line shows the level of 1/3 of the maximum amplitude of the intrinsic mode.

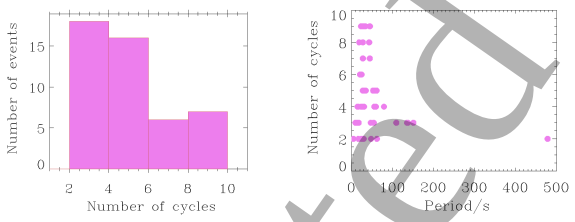

Figure 3. Left panel: Histogram of the number of oscillation cycles in the QPP detected in the solar flares produced by active region 12172/12192/12209 in September–November 2014. Right panel: Dependence of the number of oscillation cycles in QPP on the mean period.

discussion in [24]).

Nevertheless, the detection and analysis of QPP signals, including the statistical surveys [7, 8, 10, 11, 9] and automated detection techniques [10], are traditionally carried out by methods based upon the Fourier transform, for example, the windowed Fourier, wavelet analysis, Hilbert transform, and Wigner–Ville (WV) transform. This approach assumes that the signal has a harmonic shape, possibly with slowly modulated amplitude and period. Thus, its best performance is in the case of a monochromatic signal existing during the whole duration of the flare, or at least with a sufficiently large number of oscillation cycles.

In particular, frequency–time spectra obtained with the WV transform allow for the analysis of non-stationary properties of the signal. However, as the method relies on a windowed Fourier analysis, it is essentially limited to the signals with *slowly* changing frequency and power (see e.g. the 5-min solar flare pulsations with slow linear frequency drift, detected with the WV method by [25]). Another inherent shortcoming of the WV analysis is that it is adversely affected by the presence of the so-called cross (non-diagonal) terms in the covariance matrix of the input signal, leading to the meaningless redistribution of the spectral power for some frequency ranges. This becomes particularly important when the signal comprises of more than one oscillatory component, thus putting natural restrictions on its application for multi-modal and broadband QPP. Though, a QPP consisting of two quasi-monochromatic signals, one with a stationary period and the other with the period gradually increasing in time, were detected by the WV method in the radio emission of a flare on the star AD Leo [26].

In principle, wavelet analysis seems to be a suitable QPP detection and analysis tool, as it is specifically tuned to study non-stationary, localised in time, signals. However, the outcome of a wavelet transform is quite sensitive to the choice of the mother function (see, e.g. [27]). Moreover, the Morlet mother function that is commonly used in the QPP study (e.g. [7]), is not designed for accounting for the period modulation within the wavelet. Application of this technique is illustrated in the third column of Fig. 4. The top panel shows the wavelet spectrum of the full signal. The only pre-processing made was the operation of signal centring over time. The global wavelet of the signal shows its coloured nature that could be attributed to either red noise or the trend. The bottom panel shows the wavelet spectrum of the autocorrelation function of the detrended signal. The presence of a statistically significant decaying harmonic oscillatory signal with a period of about 8 minutes is clearly seen. The right column of Fig. 4 shows the global wavelet spectra. A statistically significant spectral peak occurs only in the spectrum of the autocorrelation. The second top panel shows the Fourier power spectrum of the detrended signal. The 8-min peak is above the 99% confidence level. However, the power spectrum does not allow for the study of the time variation of the signal modulation.

The Hilbert transform allows for a high-precision determination of the instantaneous amplitude and

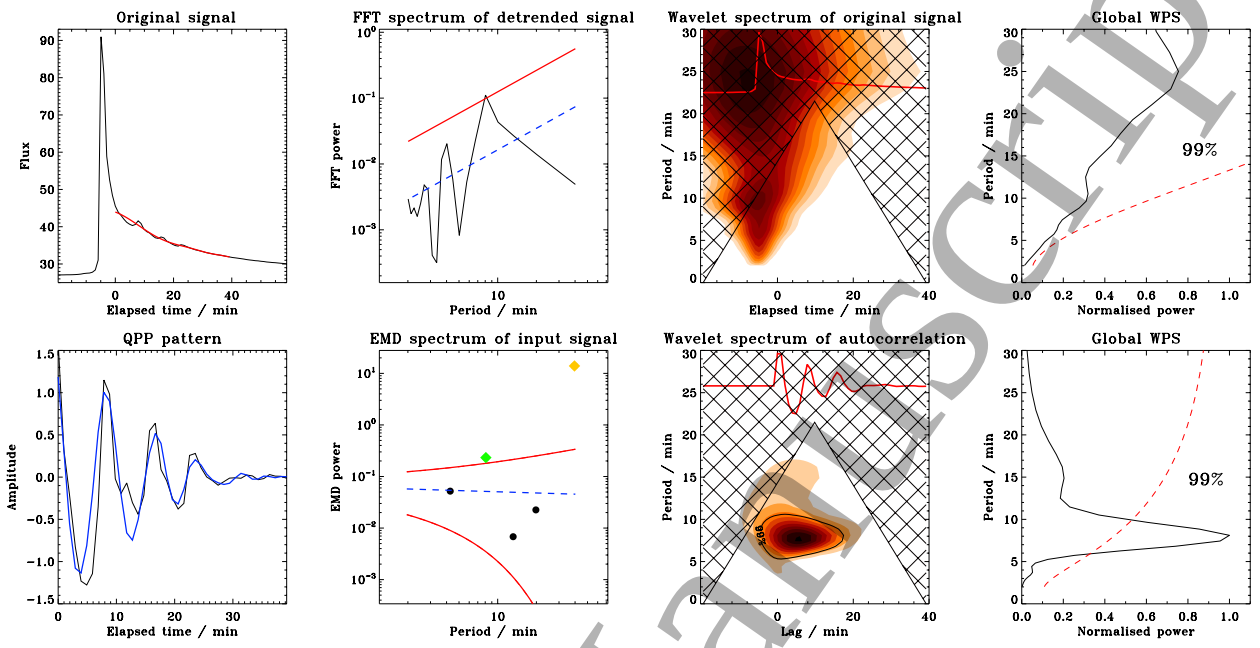

Figure 4. Example of a flare on the star KIC 9726699 (cf. Figure B8 of [12]). Clockwise from top left: Original light curve of a white light flare (black), and an overall trend of a section of the flare containing QPP, determined with EMD (red). The elapsed time starts at 18:28:48 UT on 13 March 2013, corresponding to the beginning of the flare section with QPP; Fourier power spectrum of the flare section with QPP with the overall trend subtracted (black) and its best fitting by a power law (dashed blue) with the 99% confidence interval (red) calculated based on the chi-squared, 2 degrees of freedom distribution of the noise; Morlet wavelet power spectrum of the original flare light curve. The normalised time profile of the flare is overlaid in red for comparison; Global wavelet spectra of the original (top right) and autocorrelation (bottom right) signals, obtained by integration of the corresponding wavelet power spectra over time. The red dashed lines here show the 99% significance level defined in the assumption that the background noise signal is red noise function; Morlet wavelet power spectrum of the autocorrelation function of the detrended signal (shown in red) of the original flare light curve. The black contour indicates the 99% significance level in comparison with red noise; EMD power spectrum, that is the dependence of the mean oscillation period upon the total energy density of all modes detected with EMD in the flare section indicated in the top left panel. The yellow and green diamonds indicate the overall trend and the mode with statistically significant properties, respectively. The black circles show the modes associated with noise. The red solid lines delineate the 99% confidence interval of noise with a certain value of the power law index $\alpha \approx 1$ (flicker noise) determined from the best fitting of the Fourier power spectrum. The dashed blue line shows the position of the expected mean value of the EMD modal energy density within this interval; Detrended flare section containing QPP (black) and an intrinsic mode found to be statistically significant in the EMD analysis (blue).

period. It could also be suitable for the QPP detection and analysis in the case the QPP pattern consists of several high-quality harmonic signals. In particular, it has been used in the analysis of a multi-modal QPP signal in [28]. Moreover, this technique seems to perform well in the analysis of essentially anharmonic signals (see e.g. Figs. 32–35 of [29]). However, Hilbert spectra are rather sensitive to the presence of noise, which leads to strong scattering of the instantaneous period in the spectrum (see, e.g. Fig. 2 of [28]). Another limitation of the Hilbert transform is that the analysed signal must be sufficiently narrow band to have meaningful instantaneous frequencies in the Hilbert spectrum (see the detailed discussion of this issue in Sec. 3 of [29]). Hence, the original broadband signal should be decomposed into its narrow band components before effectively processing it with the Hilbert transform.

A recently introduced method for such a reduction of the original signal is the Empirical Mode Decompo-

sition (EMD) technique that allows one to study intrinsically non-stationary oscillatory patterns, see, e.g. [30, 13] for detailed reviews. In a nutshell, the method treats the signal of interest as a superposition of many active intrinsic time scales. Operating locally and hence adaptively, it iteratively sifts these time scales from the signal thus forming a set of intrinsic mode functions (IMFs or "intrinsic modes") each of them potentially representing a certain non-stationary and anharmonic oscillatory process in the original signal. EMD has been used for the detection of non-stationary multi-modal QPP in solar (e.g., [28, 31, 32]) and stellar flares (e.g., [31, 33]). However, the full scale application of this technique requires deeper understanding of its properties and shortcomings. In particular, it is important to understand that an IMF does not necessarily represent a statistically significant oscillatory signal, like, e.g., a peak in a Fourier power spectrum indicates a statistically significant harmonic signal. An important recent advance was the creation of a robust recipe for the estimation of the statistical significance of detected intrinsic modes in the presence of white and power-law-distributed noise [34]. In this estimation it is assumed that the energy density of the intrinsic modes obtained from a pure noise is distributed by a chi-squared law with a certain number of degrees of freedom varying with the instantaneous period and colour of noise. Thus, a mode lying above a certain threshold level (confidence interval) of this distribution is considered as the mode with statistically significant properties.

Application of the EMD technique is illustrated in the first two panels of the bottom row of Fig. 4. It reveals the presence of five intrinsic modes in the original signal, one of which (with the longest time scale) represents its overall trend. Analysis of statistical significance of these modes allowed us to identify one significant mode (above 99% confidence level) with the mean oscillation period about 8 min and rapidly decaying amplitude, which nicely fits the original signal and thus represents an example of a statistically significant QPP in a stellar flare. The other three modes are seen to be statistically indistinguishable from noise with the power law index $\alpha \approx 1$ (that is pink or flicker noise), whose value was obtained from the best fitting of the Fourier power spectrum of the original signal with the overall trend subtracted (see the second panel in the top raw of Fig. 4).

2.2. The trend

The QPP signal occurs on a smooth flaring trend, e.g. the red curve in the top panel of Fig. 2, contaminated by noise. The trend could be determined by several techniques, in particular by smoothing of the light curve with a boxcar average of a specified width, or best-fitting by a guessed function, usually a low-order polynomial or an exponential decay function. However, determination of the trend by those methods is rather subjective operation, as it depends on the arbitrary choice of the smoothing width or the order of the polynomial. In addition, in the same flare the shape of the trend could be different in the emission produced by the mechanisms associated with non-thermal (e.g. in the radio, hard X-ray, gamma-ray and possibly white light bands) and thermal (e.g. in soft X-rays) emissions which are connected with each other by the Neupert effect. Obviously, detrending changes the spectrum of the analysed signal, can lead to the appearance of spurious peaks, and affects the estimation of the statistical significance. The superposition of the flaring trend and QPP could be contaminated by noise, which is often a superposition of the red and white noise [35].

Because of this, a number of recent studies avoided the problem of disentangling the flare trend and red noise by not detrending at all (e.g., [10, 35, 9]). However the flare trend does have a significant impact on the shape of flare power spectra (e.g., [32]), and as such can make QPP signals much more difficult to detect [35]. Therefore there is a huge incentive to detrend flare light curves using an analytical model, in a way that does not risk introducing artificial signal that may be misinterpreted as QPP. A number of flare light curves have a characteristic shape consisting of a sharp increase in the signal, followed by a gradual decrease, see, e.g. the empirical shape of a stellar flare determined in [36]. In addition, [37] developed an analytical model of a soft X-ray light curve of an "elementary" flare was proposed,

$$f_{\rm SXR}(t) = AC \exp\left[D(B-t) + \frac{C^2D^2}{4}\right] \times \left[\mathrm{erf}(Z) - \mathrm{erf}\Big(Z - \frac{t}{C}\Big)\right], \quad (1)$$

where A, B, C and D are constant, and $Z = (2B + C^2D)/2C$. The function $f_{\rm SXR}(t)$ is derived under assumption that the energy deposition is a Gaussian function of time, while the energy dissipation by radiation and thermal conduction is exponential. This function reproduces the majority of powerful stellar flares, while light curves of less powerful solar flares are often different, see, e.g. Fig. 1 and 2. However this function could be generalised under the assumption that energy dissipation via radiative and conductive processes happens on different timescales, and therefore two terms for the energy losses could be included, corresponding to radiative and conductive cooling. In addition, other profiles of the energy deposition function could be considered. In the modelling of specific flares, the constants should be

determined by a best-fitting method. Fig. 5 shows that it could be difficult to distinguish Fourier power spectra of model trends from the red noise spectrum. Detrending techniques that are less subjective, are the use of an autocorrelation function of the light curve (see, e.g. [7]), or the lowest intrinsic mode determined by EMD (see, e.g. [32]).

2.3. Anharmonicity

As it has already been pointed out in [18], individual cycles of QPP are often of an essentially anharmonic shape, in particular of a symmetric triangle. Fig. 6 gives an example of such a QPP pattern. Another frequently detected feature is a double sub-peak [38]. Such an essentially anharmonic signal shape could be produced either by a superposition of several oscillatory harmonics, or by nonlinearity. In the former case, the observed signal could be produced by a summative effect of various nearly-harmonic MHD modes excited in the flare site (e.g., [28]). However, in this scenario the shape of the signal should evolve in time because of the variation of the individual modes. In other words, different cycles of the QPP should have different shapes.

The latter interpretation has not received sufficient attention in the data analysis so far. But nonlinear effects and non-linear mechanisms are often addressed in theoretical studies, see, e.g., the magnetic tuning fork mechanism [39], and the oscillatory coalescence of current-carrying magnetic flux tubes [40]. In particular, the symmetric triangular shape could appear as an absolute value of a sawtooth wave that could be readily formed by a quadratic nonlinearity, typical for weakly nonlinear magnetoacoustic waves. Another possibility is to produce a triangle oscillation is an integral of a square wave that could be readily produced, e.g., by the nonlinear evolution of a standing acoustic wave [41].

The mechanisms for QPP based on the concept of "magnetic dripping", i.e. self-oscillatory mechanisms, should produce signals of the relaxation shape, with the high and low amplitude phases of different duration. This property, if confirmed by theoretical modelling, could be searched for in the data.

3. Need for the classification of QPP

The vast amount of information gained by the research community about QPP in various case studies of solar and stellar flares demonstrates a broad variety of the QPP durations, q-factors, period drifts, characteristic anharmonic shapes, etc., as well as the phases of the flare. Thus, it is likely that QPP with different properties are caused by different physical mechanisms. QPP that belong to different (while yet not identified) classes should have different relationships between QPP parameters, as well as parameters of the flare and the host active region. In other words, statistical analysis of QPP is complicated by the lack of established classification of the QPP types. The same problem limits the use of QPP for the plasma diagnostics that should be based on the unequivocal interpretation of the observed QPP pattern with a certain physical mechanism. The broad variety of QPP properties suggests the need for a common classification, similar to the classifications of, for example, solar radio bursts or magnetospheric magnetic pulsations (see Sec. 3.2).

3.1. Decaying harmonic QPP

One obviously distinct class of QPP is a rapidly decaying harmonic oscillation, see, for example, Fig. 4. The typical signature of this class is the relatively long oscillation period, typically greater than one minute, localisation of those QPP in the decaying phase of the flare, and an almost harmonic signal that decays very rapidly, typically in a few oscillation cycles. QPP of this class are usually detected in the EUV, soft X-ray and microwave light curves of solar flares, and soft X-ray and white-light emission of stellar flares. Very similar oscillatory patterns are detected as rapidly decaying oscillatory Doppler shifts of the EUV emission lines associated with a hot, > 6 MK plasma in the solar corona (see [42] for a comprehensive review of so-called "SUMER" oscillations). Theoretical modelling demonstrated that SUMER oscillations are likely to be slow magnetoacoustic oscillations in coronal loops. Moreover, this mechanism can explain the quasi-periodic progression of energy release sites along the neutral line in two-ribbon flares [43].

In this class of QPP, the oscillation damping time is empirically found to scale linearly with the period. This result is unexpected, as the dissipative mechanisms that affect coronal magnetoacoustic waves: thermal conduction, viscosity and resistivity, should lead to the quadratic dependence. Intriguingly, this unusual linear scaling has been found in soft X-ray QPP in both solar and stellar flares [31], as well as in the SUMER oscillations directly observed in the Doppler shift, and hence is a robust empirical result. Usually, the damping time is determined from the best-fitting exponential decay function. But, it has been shown that in some cases a Gaussian decay is more appropriate [12, 32]. Physical mechanisms responsible for the Gaussian damping of slow magnetoacoustic waves in the corona have not been identified yet, but are known in the case of coronal fast magnetoacoustic waves of the kink symmetry [44].

In the case of SUMER oscillations, it is usually possible to estimate the apparent (reduced by the

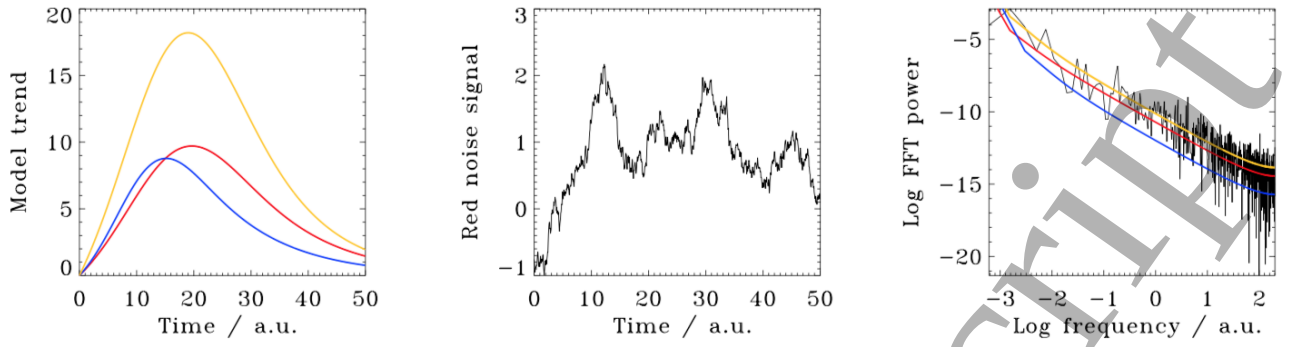

Figure 5. Left panel: Flare trends constructed by the model of [37] with $A = 1.2$, $B = 12.0$, $C = 11.9$ and $D = 0.08$ (red curve); $A = 1.2$, $B = 8.6$, $C = 8.7$ and $D = 0.08$ (blue curve), and $A = 2.4$, $B = 12.0$, $C = 12.0$ and $D = 0.08$ (yellow curve). Central panel: An example of a red noise signal. Right panel: Fourier power spectra of the signals shown in the left and right panel.

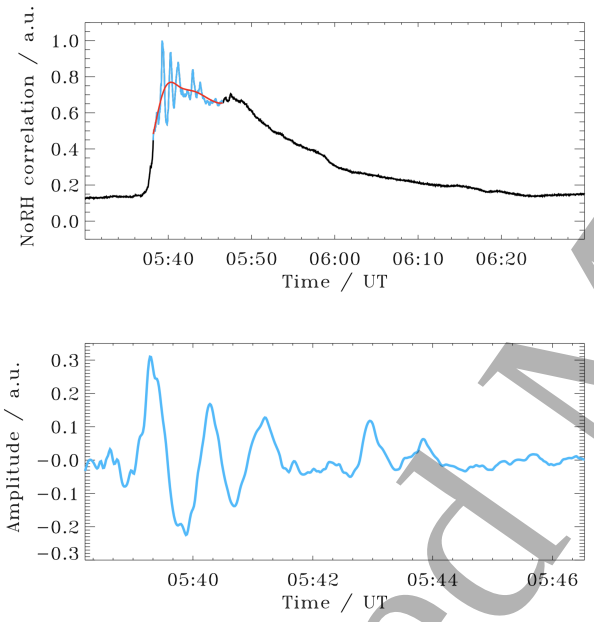

Figure 6. Solar flare SOL2017-09-04T05:39:15, as seen in the correlation curve of the Nobeyama Radioheliograph at 17 GHz. The section of the flare, containing a well pronounced QPP is shown in blue. Its slowly varying trend determined with EMD is shown by the red line. Bottom: The flare section indicated in blue in the top panel with the overall trend and higher-frequency components subtracted, showing the presence of a well pronounced QPP pattern of a symmetric triangular shape.

projection effect) amplitude of oscillatory flows by the Doppler shift of emission lines. Using this information, [41] noticed that the damping times of SUMER oscillations decrease with the oscillation amplitude. It indicates the nonlinear nature of the phenomenon. In particular, it could be connected with the formation of slow magnetoacoustic shocks. However, in that case, the oscillatory signal has a characteristic square shape, which has not been found in observations. Recently, rapidly decaying acoustic oscillations induced by an impulsive energy release were found in the infinite field modelling [23] that reduces slow magnetoacoustic waves to the pure acoustic. Furthermore, some additional physical processes, for example the misbalance of the radiative losses, thermal conduction and unspecified background heating of the coronal plasma could either significantly increase or decrease the damping time [45].

3.2. Similarity of QPP in flares and geomagnetic Pi pulsations

An intensively studied geophysical phenomenon, pulsations of the Earth's magnetic field, have a number of interesting similarities with QPP in flares. Of a specific interest are the geomagnetic pulsations of the Pi class, "irregular pulsations". This similarity is illustrated by Fig. 7 that shows an example of a Pi2 pulsation signal, processed by the same tools as a QPP shown in Fig. 4. Moreover, theoretical interpretations of geomagnetic irregular pulsations operate by the same models as used in the QPP study, namely the mechanisms based upon various resonances of MHD waves, and repetitive regimes of magnetic reconnection (see, e.g. [13]).

There is an elaborated and commonly accepted classification of geomagnetic pulsations (see [46] for a comprehensive review). This classification is based on several observables, namely the pulsation period, number of pulsations in the signal, period drifts, etc. In particular, in the Pi class, different subclasses are identified on the basis of distinct signatures of their dynamical Fourier or wavelet spectra, see Table 1 of [46]. Identification of specific classes and subclasses is important for revealing specific physical mechanisms for the pulsations.

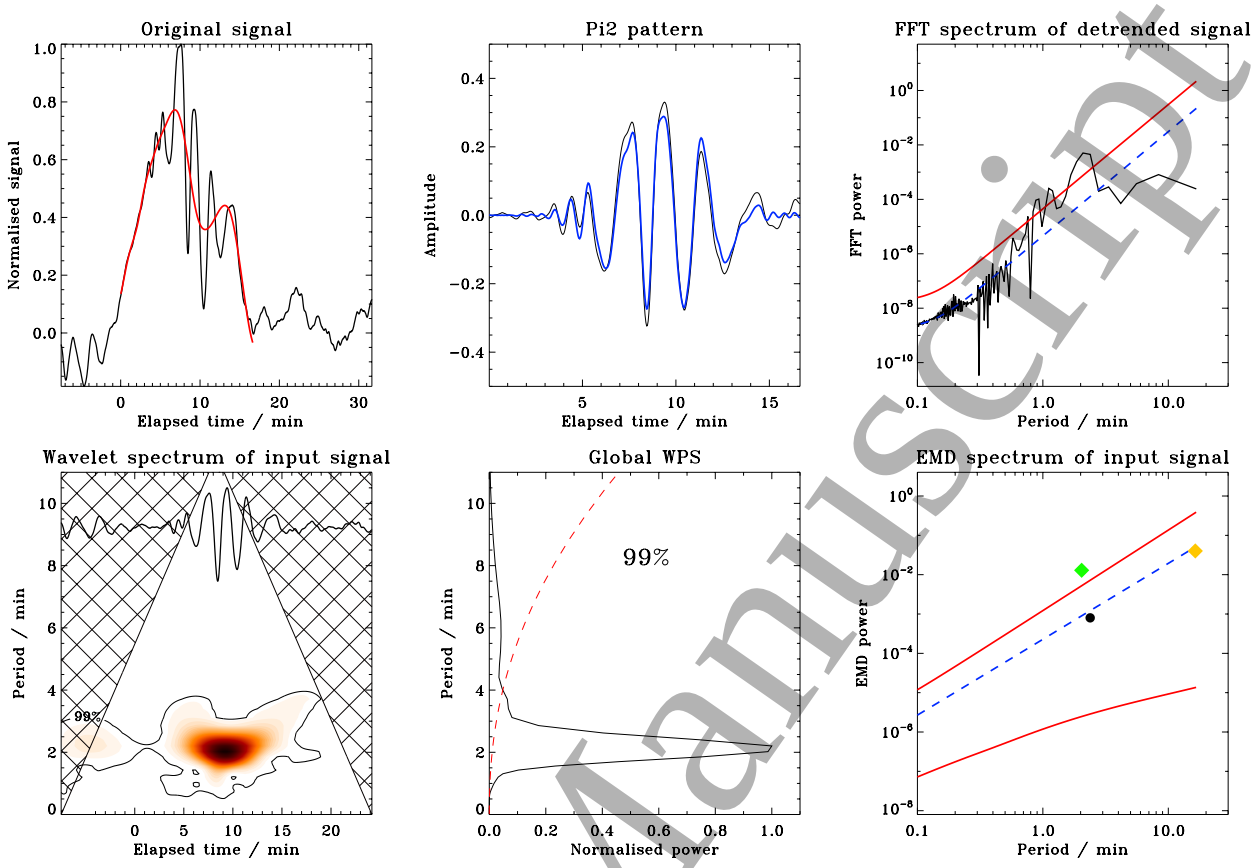

Figure 7. Example a magnetospheric Pi2 pulsation on 25 February 2008 at about 10:30 UT, recorded by the ground magnetometer data of the high-latitude station FSMI (cf. Fig. 3 of [43], courtesy of Dr A. Keiling). Clockwise from top left: A normalised signal. The red line shows a slowly-varying trend of the signal section with the Pi2 pattern, obtained as the lowest-frequency mode in the EMD analysis; Detrended signal section containing Pi2 (black) and an intrinsic mode found to be statistically significant in the EMD analysis (blue); Fourier power spectrum of the signal section with Pi2 with the overall trend subtracted (black) and its best fitting by a power law (dashed blue) with 99% confidence interval (red) of a chi-squared distribution with 2 degrees of freedom; EMD power spectrum of the signal section indicated in the top left panel, with the 99% confidence interval (red) of noise with the power law index $\alpha \approx 3$ determined from the best fitting of the Fourier power spectrum. The expected mean values of the EMD modal energy density within this confidence interval are shown by the dashed blue line; Global wavelet spectrum of the original signal with the overall trend subtracted, obtained by integration of the corresponding wavelet power spectrum over time. The red dashed line here shows the 99% significance level defined in the assumption that the background noise signal is the red noise function; Morlet wavelet power spectrum of the original signal with the overall trend subtracted. The normalised time profile of the detrended signal is overlaid in black for comparison. The black contours indicate the 99% significance level in comparison with red noise. The notations are similar to those in Fig. 4.

4. Discussion and Conclusions

In this brief review we discussed non-stationary properties of QPP in flares. Theoretical models of the QPP phenomenon in solar and stellar flares predict its transient and modulated nature. The application of analytical tools designed for the study of non-stationary signals, such as wavelet transform and EMD, allows for studying this property. The use of spatially resolving observations of solar flares would reveal correlations of variations of properties of QPP with variations of physical and geometrical parameters of flaring active regions.

The non-stationarity of QPP signals could provide a basis for their classification. The classification is needed for revealing the mechanisms responsible for QPP, and the use of QPP for seismological diagnostics of flaring plasmas. The classification should be based not only on the values of mean periods, as it was done in [47] and [15], but also on the non-stationary signatures, such as amplitude modulation, period drifts, number of oscillation cycles, and signal shape. Another important feature of QPP that could be used in their classification is the mean oscillation period normalised by the flare duration, or the duration of its impulsive phase. We could identify one clearly distinct

class of QPP, the decaying harmonic oscillations in the decay phase of the flare, which are interpreted as slow magnetoacoustic oscillations in the flaring loops. QPP of these class are common in solar and stellar flares. Perhaps, another class are QPP appearing as short trains of pulsations of the symmetric triangular shape.

We also pointed out the similarity of QPP in flares and geomagnetic Pi pulsations, which has not been exploited so far, but it clearly provides us with a ground for the interdisciplinary knowledge transfer. In particular, the experience in the signal processing techniques gained in QPP studies, for example in EMD, would be of interest for magnetospheric applications. Another topic for the knowledge transfer could be the theories of oscillatory and self-oscillatory mechanisms designed independently in the coronal and magnetospheric research communities. The elaborated classification system of geomagnetic Pi pulsations could be used as an example for the classification of QPP in flares.

Acknowledgments

This study was supported by the STFC consolidated grant ST/P000320/1 (VMN, DYK), the BK21 plus program through the National Research Foundation funded by the Ministry of Education of Korea (VMN, DHL), the Royal Society International Exchanges grant IEC\R2\170056, and partly by RFBR according to the research project N17-52-10001 (EK). We also acknowledge support from the International Space Science Institute for the team "Quasi-periodic Pulsations in Stellar Flares: a Tool for Studying the Solar-Stellar Connection" and the International Space Science Institute Beijing for the team "MHD Seismology of the Solar Corona".

References

[1] Shibata K and Magara T 2011 *Living Rev. Solar Phys.* **8** 6
[2] Benz A O 2017 *Living Reviews in Solar Physics* **14** 2
[3] Davenport J R A 2016 *Astrophys. J.* **829** 23
[4] Notsu Y, Shibayama T, Maehara H, Notsu S, Nagao T, Honda S, Ishii T T, Nogami D and Shibata K 2013 *Astrophys. J.* **771** 127
[5] Parks G K and Winckler J R 1969 *Astrophys. J. Lett.* **155** L117
[6] Namekata K, Sakaue T, Watanabe K, Asai A, Maehara H, Notsu Y, Notsu S, Honda S, Ishii T T, Ikuta K, Nogami D and Shibata K 2017 *Astrophys. J.* **851** 91
[7] Kupriyanova E G, Melnikov V F, Nakariakov V M and Shibasaki K 2010 *Solar Phys.* **267** 329–342
[8] Simões P J A, Hudson H S and Fletcher L 2015 *Solar Phys.* **290** 3625–3639
[9] Dominique M, Zhukov A N, Dolla L, Inglis A and Lapenta G 2018 *Solar Phys.* **293** 61
[10] Inglis A R, Ireland J, Dennis B R, Hayes L and Gallagher P 2016 *Astrophys. J.* **833** 284
[11] Pugh C E, Nakariakov V M, Broomhall A M, Bogomolov A V and Myagkova I N 2017 *Astron. & Astrophys.* **608** A101
[12] Pugh C E, Armstrong D J, Nakariakov V M and Broomhall A M 2016 *Mon. Not. Roy. Astron. Soc.* **459** 3659–3676
[13] Nakariakov V M, Pilipenko V, Heilig B, Jelínek P, Karlický M, Klimushkin D Y, Kolotkov D Y, Lee D H, Nisticò G, Van Doorsselaere T, Verth G and Zimovets I V 2016 *Space Sci. Rev.* **200** 75–203
[14] McLaughlin J A, Nakariakov V M, Dominique M, Jelínek P and Takasao S 2018 *Space Sci. Rev.* **214** 45
[15] Nakariakov V M and Melnikov V F 2009 *Space Sci. Rev.* **149** 119–151
[16] Uzdensky D A, Loureiro N F and Schekochihin A A 2010 *Physical Review Letters* **105** 235002
[17] Nishizuka N and Shibata K 2013 *Physical Review Letters* **110** 051101
[18] Nakariakov V M, Inglis A R, Zimovets I V, Foullon C, Verwichte E, Sych R and Myagkova I N 2010 *Plasma Phys. Controlled Fusion* **52** 124009
[19] Van Doorsselaere T, Kupriyanova E G and Yuan D 2016 *Solar Phys.* **291** 3143–3164
[20] Guo M Z, Chen S X, Li B, Xia L D and Yu H 2016 *Solar Phys.* **291** 877–896
[21] Russell A J B, Simões P J A and Fletcher L 2015 *Astron. & Astrophys.* **581** A8
[22] Hayes L A, Gallagher P T, Dennis B R, Ireland J, Inglis A R and Ryan D F 2016 *Astrophys. J. Lett.* **827** L30 (*Preprint* 1607.06957)
[23] Reale F, Lopez-Santiago J, Flaccomio E, Petralia A and Sciortino S 2018 *Astrophys. J.* **856** 51
[24] Boashash B 1992 *IEEE Proceedings* **80** 520–538
[25] Kislyakov A G, Zaitsev V V, Stepanov A V and Urpo S 2006 *Solar Phys.* **233** 89–106
[26] Zaitsev V V, Kislyakov A G, Stepanov A V, Kliem B and Furst E 2004 *Astronomy Letters* **30** 319–324
[27] De Moortel I and Hood A W 2000 *Astron. & Astrophys.* **363** 269–278
[28] Kolotkov D Y, Nakariakov V M, Kupriyanova E G, Ratcliffe H and Shibasaki K 2015 *Astron. & Astrophys.* **574** A53
[29] Huang N E, Shen Z, Long S R, Wu M C, Shih H H, Zheng Q, Yen N C, Tung C C and Liu H H 1998 *Proceedings of the Royal Society of London Series A* **454** 903–998
[30] Huang N E and Wu Z 2008 *Reviews of Geophysics* **46** RG2006
[31] Cho I H, Cho K S, Nakariakov V M, Kim S and Kumar P 2016 *Astrophys. J.* **830** 110
[32] Kolotkov D Y, Pugh C E, Broomhall A M and Nakariakov V M 2018 *Astrophys. J. Lett.* **858** L3
[33] Doyle J G, Shetye J, Antonova A E, Kolotkov D Y, Srivastava A K, Stangalini M, Gupta G R, Avramova A and Mathioudakis M 2018 *Mon. Not. Roy. Astron. Soc.* **475** 2842–2851
[34] Kolotkov D Y, Anfinogentov S A and Nakariakov V M 2016 *Astron. & Astrophys.* **592** A153
[35] Pugh C E, Broomhall A M and Nakariakov V M 2017 *Astron. & Astrophys.* **602** A47
[36] Davenport J R A, Hawley S L, Hebb L, Wisniewski J P, Kowalski A F, Johnson E C, Malatesta M, Peraza J, Keil M, Silverberg S M, Jansen T C, Scheffler M S, Berdis J R, Larsen D M and Hilton E J 2014 *Astrophys. J.* **797** 122
[37] Gryciuk M, Siarkowski M, Sylwester J, Gburek S, Podgorski P, Kepa A, Sylwester B and Mrozek T 2017 *Solar Phys.* **292** 77
[38] Tajima T, Sakai J, Nakajima H, Kosugi T, Brunel F and Kundu M R 1987 *Astrophys. J.* **321** 1031–1048
[39] Takasao S and Shibata K 2016 *Astrophys. J.* **823** 150
[40] Kolotkov D Y, Nakariakov V M and Rowlands G 2016 *Phys. Rev. E* **93** 053205
[41] Verwichte E, Haynes M, Arber T D and Brady C S 2008

Astrophys. J. **685** 1286–1290
[42] Wang T 2011 *Space Sci. Rev.* **158** 397–419
[43] Nakariakov V M and Zimovets I V 2011 *Astrophys. J. Lett.* **730** L27
[44] Pascoe D J, Hood A W, De Moortel I and Wright A N 2013 *Astron. & Astrophys.* **551** A40
[45] Nakariakov V M, Afanasyev A N, Kumar S and Moon Y J 2017 *Astrophys. J.* **849** 62
[46] Saito T 1978 *Space Sci. Rev.* **21** 427–467
[47] Aschwanden M J 1987 *Solar Phys.* **111** 113–136